Proceedings of the International Symposium for Bridge Earthquake Engineering
in Honor of Retirement of Professor Kazuhiko Kawashima, Tokyo, Japan, March 15, 2013

# MULTI-HAZARD RESISTANT HIGHWAY BRIDGE PIERS HAVING CONCRETE-FILLED STEEL TUBE

Shuichi FUJIKURA[1] and Michel BRUNEAU[2]

[1] Senior Engineer, ARUP North America, Los Angeles, CA, USA
shuichi.fujikura@arup.com
[2] Professor, Department of Civil, Structural and Environmental Engineering, University at Buffalo, Buffalo, NY, USA, bruneau@buffalo.edu

**ABSTRACT**: This paper presents the development and experimental validation of a multi-hazard bridge pier concept, i.e., a bridge pier system capable of providing an adequate level of protection against collapse under seismic and blast loading. A multi-column pier-bent with concrete-filled steel tube (CFST) columns is the proposed concept, and the adequacy of this system is experimentally and analytically investigated under blast loading.

**Key Words**: Blast loads, Bridges, Piers, Columns, Steel, Concrete-filled steel tube, Dynamic analyses, Multi-hazard.

## INTRODUCTION

Terrorist attacks such as the one on the Alfred P. Murrah Federal Building in Oklahoma City (1995) and the one on the tallest towers of the World Trade Center in New York City (2001) are examples of the fact that the destruction of civil engineering structures has become one of the means employed by terrorists to achieve their objectives. Although bridge structures in North America have not been attacked so far, the terrorist threats received by the state of California to its main suspension bridges and the detailed shots of the Golden Gate and Brooklyn bridges found among the possessions of terrorists captured in Spain indicate that bridge structures are being considered as potential targets by terrorist organizations (Williamson and Winget 2005). The terrorist threat on bridges, and on the transportation system as a whole, has been recognized by the engineering community and public officials, which resulted in the recent publication of a number of documents addressing this concern (see, for instance, FHWA 2003).

There is a need to develop bridge structural systems capable of providing an adequate level of protection against intentional blast loads. Any blast-resistant structural system must still be able to perform satisfactorily under all of the other loads acting on bridge structures. In this regard, it is interesting to note that there are some important similarities between seismic and blast effects on bridge structures: both major earthquakes and terrorist attacks are rare events, and, due to economic considerations, most of the energy imposed on structural members by these events is dissipated through inelastic deformations rather than elastically absorbed. Given the fact that: (a) current codes require that bridge structures be designed for some level of seismic action in most states in the US; and (b) blast and seismic loads often control the design, there is a need for structural systems capable of performing equally well under both seismic and blast loads.

This paper presents the results of a research project conducted to develop and experimentally validate such a multi-hazard bridge pier concept, i.e., a bridge pier system capable of providing an adequate level of protection against collapse under both seismic and blast loading, and whose structural, construction and cost characteristics are not significantly different from those of the pier systems currently found in typical highway bridges in the US. The proposed pier system is a pier-bent where CFST columns frame into beams made up of C-shape steel sections embedded in the fiber-reinforced concrete foundation and pier cap. Also, two different analytical methods have been adopted to replicate the behavior of the tested CFST columns subjected to blast loading, namely a simplified analysis using an equivalent SDOF system and a fiber-based dynamic analysis. The maximum residual deformations obtained from these two blast analyses are compared with the experimental results.

The multi-hazard bridge pier-bent concept proposed in this study is intended for use in typical highway bridges. Although the terrorist threat to this type of bridges is usually assumed to be of lesser magnitude than that assigned to large signature bridges, the threat, especially to the ones strategically located, is nevertheless real and worthy of consideration (Winget et al. 2005). There are many possible courses of action by which terrorists might intend to destroy a bridge structure. The bridge pier-bent concept proposed was developed considering only one type of terrorist threat: the detonation of explosives located inside a small vehicle placed below the deck at close distance to the pier. Other possible courses of action, such as the detonation of hand-placed explosives and collisions using large vehicles, were not considered. Note that for security reasons, some key details of this blast-related study are withheld from this paper. More specifically, the numerical values of some key quantities are not provided but presented in terms of parameters.

## CFST COLUMNS BRIDGE PIER-BENT CONCEPT

Preliminary analysis and existing literature (e.g. Winget et al. 2005) indicate that the combined effects of spalling and cratering, possibly breaching control the design of substructure concrete members subjected to close-in blast loading. In this context, spalling and cratering are disengagement of the concrete at back and front side of the member, respectively, and breaching is punching through the full concrete thickness (UFC 2004). The behavior of concrete members under blast loading could be substantially improved if these behaviors could be somehow prevented. In that perspective, encasing concrete in a steel shell would seem to be an adequate approach to provide blast-resistant piers. The addition of steel jackets has been shown to be a viable strategy for the seismic retrofit of concrete bridge pier columns (Priestley et al. 1996). However, here, using such a jacket alone was calculated to be insufficient to provide adequate resistance to the large shear forces that develop at the base of piers subjected to blast loads. As such, using a fully composite concrete-filled steel tube continuous into the footing was found to be a more appropriate solution. Therefore, the pier concept considered in this study is a multi-column pier-bent with concrete-filled steel tube (CFST) columns. Tests carried out by Marson and Bruneau (2004) for the purpose of seismic applications showed that CFST columns subjected to cyclic loading exhibit good energy-dissipation capabilities and stable hysteretic behavior up to a drift level equal to 7 %. A possible implementation of this concept is schematically shown in Fig. 1(a). The foundation beam consists of concrete-embedded C-channels linked to the columns through steel plates. This connection concept is schematically illustrated in Fig. 1(b). This type of foundation beam performed successfully in the tests by Marson and Bruneau (2004) in that it allowed the composite columns to develop their full moment capacity. Conceptually, the channels are designed to resist the full composite strength of the columns, and the concrete at the foundation beam does not need any reinforcement for strength purposes (fiber concrete is however recommended to prevent cracking of the concrete and subsequent water infiltration into the footing).

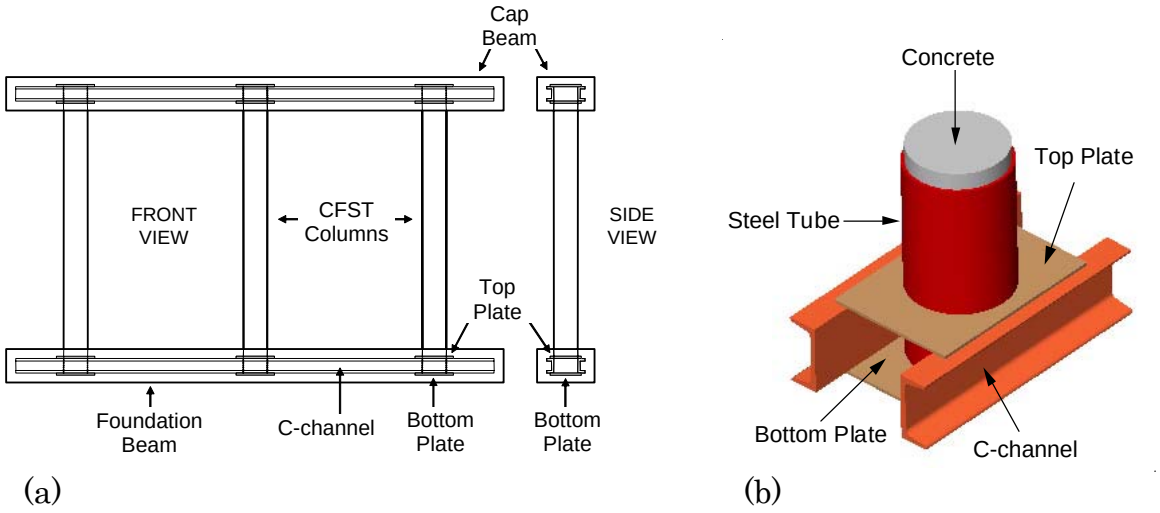


Fig. 1 Multi-column pier-bent made up of CFST columns: (a) General description (b) Details of column-to-foundation beam connection

## DESIGN OF MULTI-HAZARD BRIDGE PIERS

Preliminary work included the examination of several different structural configurations of bridge piers and potential bridge bent systems, to identify some systems deemed most appropriate in meeting the objectives of this research. In all cases, bents were assumed part of a typical 3-span continuous highway bridge located in an area of moderate seismic activity.

A pier-bent design concept consisting of CFST columns linked by a cap-beam proved to be more satisfactory, and was found possible using available tube sections (Bruneau and Marson 2004; Marson and Bruneau 2004). It was found that material effectiveness was highest for piers having the highest diameter-to-thickness (D/t) ratio. CFST columns with cross-sections of 16" diameter were found to provide adequate blast and seismic resistance during the design process. These CFST columns are smaller than the typical 3'-diameter reinforced concrete pier column, but expected to perform significantly better under blast loads. This type of structural member was deemed likely to be accepted in practice (and incidentally is helpful in fulfilling the objective of accelerated construction). This structural configuration was therefore selected for experimental verification of its blast resistance.

## MULTI-HAZARD RESISTANT BRIDGE PIER TESTS SUBJECTED TO BLAST LOADING

To verify/validate blast performance of CFST bridge piers, a series of blast tests of 1/4 scale bridge piers was conducted at the U.S. Army Corps of Engineers Research Facility in Vicksburg, Mississippi (Fujikura et al. 2007). Two identical specimens (Bent 1 and Bent 2) were constructed and tested. Each specimen consisted of three CFST columns with different diameters: D = 102 mm (4 in), 127 mm (5 in) and 152 mm (6 in), connected to a steel beams embedded in the cap-beam and foundation beam (Fig. 2). Fig. 3 shows a general photograph of the specimens' setup. The bent frames were braced in what would correspond to the bridge longitudinal direction at the level of the cap-beams. A reaction frame was built for this purpose. The cap-beams were not connected to the frame but in contact with the frame, such as to support the force from the cap-beam. This allowed properly modeling the longitudinal fixity provided by the inertia effect of the superstructure without preventing the rotation at the top of the bent. A summary of the experimental cases is presented in Table 1 along with test and analysis results. Exact values of charge weights and standoff distances are normalized and expressed in functions of W and X, respectively, for security reasons. Note that each column in the bent was tested successively as if it was a part of a regular bent. The CFST columns exhibited a

ductile behavior under blast loadings, and the experimentally obtained maximum residual deformations of the columns are presented in Table 1.

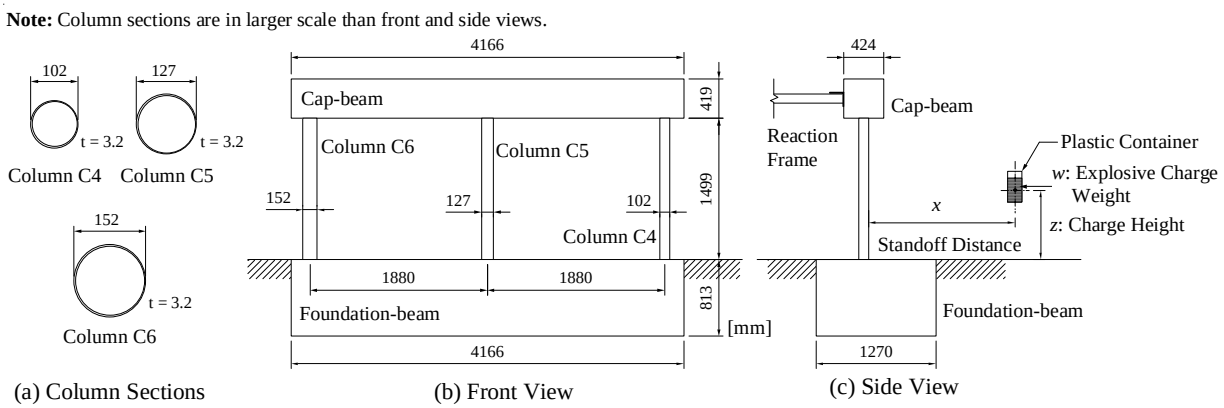


Fig. 2 Experimental specimens and explosive charge scenario

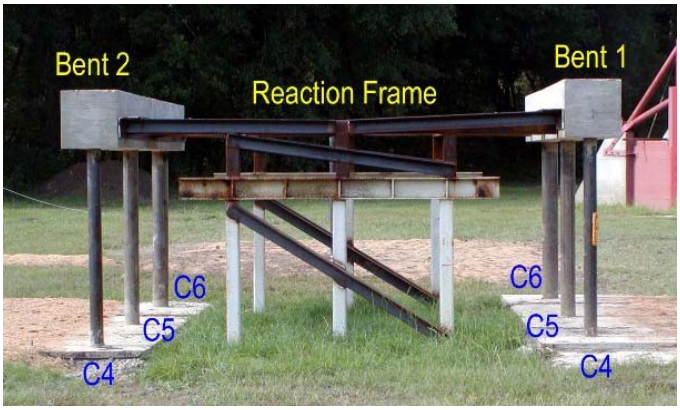


Fig. 3 Test setup

Table 1 Summary of experimental cases, and test and analytical results

| | | Objective | Blast Parameters | | | Test Results | Analysis Results |
|---|---|---|---|---|---|---|---|
| Test Num. | Col. | | *w* | *x* | *z* (m) | Residual Displ. (mm) | $\beta$ |
| 1 | C4 | Preliminary | 0.1 W | 3 X | 0.25 | 0 | --- |
| 2 | C4 | Maximum deformation | 0.55 W | 3 X | 0.75 | 0 | --- |
| 3 | C4 | | W | 2 X | | 30 | 0.472 |
| 4 | C6 | | | 1.1 X | | 46 | 0.458 |
| 5 | C5 | | | 1.3 X | | 76 | 0.447 |
| 6 | C4 | | | 1.6 X | 0.25 | 24 | 0.465 |
| 7 | C4 | Fracture of steel shell | | 0.6 X | | 395 | --- |
| 9 | C6 | | | 0.8 X | | 45 | 0.440 |
| 10 | C5 | | | 0.8 X | | 100 | 0.417 |

## EXPERIMENTAL OBSERVATIONS

Maximum deformations of Tests 3 to 5 (mid blast height cases) as shown in Table 1 were observed at the same height as the blast charge. Fig. 4(a) shows Column C5 after Test 5. Many pits and a notch were observed on the surface of the column around the height of the blast charge, as seen in Fig. 4(b). These marks can be attributed to debris impacts, particularly to the disk attached at the mid-height of the blast charge container as it hit the column during the explosion, but these minor local effects were of no impact on the results. No spalling of the concrete was observed at the cap-beam and foundation-beam as a result of the blast pressures. Inspection of core concrete after removal of half of the steel shell (Fig. 4(c)) showed that cracks occurred at column mid-height on the tension side. In addition, some cracks developed at both the top and bottom of the column on the tension side of the negative moment region due to the rigid boundary conditions. It should be added that although the cap-beams were not fixed to the reaction frames, the rotation of the cap-beam was partly restrained by the torsion resistance of the cap-beam and the other two columns in the pier-bent.


Fig. 4 Column photos: C5 after Test 5

Test 7 was conducted as a retest of Column C4, which had already experienced inelastic deformations in Test 6. The column was blown up from the bent by the explosion. In Tests 9 and 10, the blast charge was set on the side of the bent rather than on the front. This was done because it was desired to investigate a boundary condition at the top of the columns different from the one for Test 1 through Test 7. Therefore, the column boundary condition in Test 9 and Test 10 was considered to be rigid, i.e. fixed-fixed. Fig. 5(a1) and (a2) show Column C6 after Test 9 and the damage to the foundation beam. Fig. 5(b1) shows Column C5 after Test 10. Buckling of the steel tube was observed near the height where maximum deformation occurred as seen in Fig. 5(b3). The fracture of the steel was observed halfway around the base of the column as shown in Fig. 5(b2). The crater into the foundation reached the embedded C-channel connection.


Fig. 5 Column photos: (a) C6 after Test 9 and (b) C5 after Test 10

## SIMPLIFIED BLAST ANALYSIS BY EQUIVALENT SDOF

The simplified analysis procedure introduced in this study is commonly used in blast resistant design. The analysis procedure considers an equivalent SDOF system having an elastic-perfectly-plastic behavior, and assumes that all the energy imparted to the system by the blast loading is converted into internal strain energy. The key assumption of this analysis method is that real structures or components, which are multi-degree of freedom systems, can be represented by a SDOF lumped-mass system (often called an equivalent SDOF system). Although this equivalent system cannot provide the detailed response of the structure, it is enough to calculate the response at one particular point of the structure; typically the point where the maximum deformation occurs in the system chosen for design. The equation of motion for an equivalent SDOF system is written as:

$$K_{LM} M \ddot{x} + K x = P(t) \tag{1}$$

where $K_{LM}$ is the load-mass factor and $M$, $K$ and $P(t)$ are the mass, stiffness and load of the real structure, respectively. The load-mass factor, $K_{LM}$, is obtained by equating the energies of the real structure and the equivalent SDOF system. Note that the damping component is typically neglected when calculating response under blast loading since one cycle of response develops (Smith and Hetherington 1994; Mays and Smith 1995).

Structural response under blast loading depends on the response time of the structure relative to the duration of the explosion. USDA (1990) categorized the relationship between these two parameters into three design ranges, which are impulsive load, pressure-time load (also called dynamic load) and pressure load (also called quasi-static load). For the cases considered herein, where the blast load duration is much shorter than the pier column's natural periods of response, the design will typically fall within the impulsive loading category. Therefore, the energy imparted to the structural system by blast loading is considered an impulsive loading. Using the equivalent SDOF analysis method, the maximum response to an impulsive load is obtained by assuming that all the energy imparted to the system by the blast loading is converted into internal strain energy. Accordingly, by equating the kinetic energy delivered by the impulse load and the strain energy stored in the elastic-perfectly-plastic system, the maximum deformation, $X_m$, of the equivalent SDOF system due to impulsive-type blast loading is given by:

$$X_m = \frac{1}{2}\left( \frac{i^2}{K_{LM}\ m\ r_u} + X_E \right) \tag{2}$$

where $X_E$ is the elastic deflection, $i$ is the impulse, and $m$ and $r_u$ are the mass and ultimate resistance of the column per unit length, respectively (Mays and Smith 1995).

## BLAST LOADING FOR SIMPLIFIED ANALYSIS

To calculate the maximum deformation by Eq. (2), the equivalent uniform impulse per unit length, $I_{eq}$, is used for $i$ and calculated by:

$$I_{eq} = \beta\ D\ i_{eq} \tag{3}$$

where $i_{eq}$ is the equivalent uniform impulse per unit area, $D$ is the column diameter and $\beta$ is the factor to account for the reduction of pressures on the column due to its circular shape. Since the ratio of the pressure at a given angle of incidence to that at any other angle is not a constant but a function of the magnitude of the blast pressures, the value of $\beta$ is a function of both time and space. However, in order to simplify the analysis, it was decided to adopt a constant value of $\beta$. The quantity $i_{eq}$ was calculated by:

$$i_{eq} = \frac{\int_0^H i(z)\,\phi(z)\,dz}{\int_0^H \phi(z)\,dz} \tag{4}$$

where $i(z)$ indicates the variation of impulse per unit area along the height of the column and $\phi(z)$ is the normalized deflected shape of the column. In this analysis, $i(z)$ was taken as the envelop of maximum impulse (per unit area) at any time along the height of the column. Values of $i(z)$ were calculated using the program Bridge Explosive Loading (BEL 2004). BEL generates airblast pressures considering reflections of the blast wave on the deck and on the ground. The normalized deflected shape, $\phi(z)$, was taken as inelastic deformations after plastic hinging. The shape was defined by rigid-link members between plastic hinges assuming that an in-span hinge develops at the height of a blast charge and that other hinges form at both top and base of a column.

## COMPARISON WITH SIMPLIFIED ANALYSIS FOR COLUMN TESTS

Experimentally obtained maximum plastic deformations of the piers were compared with the ones that can be calculated using simplified method of analysis. These simplified analyses were conducted using the strength values obtained from the compression tests of concrete cylinders and the tensile tests for the steel tubes. Following the approach presented previously by calibrating analysis with the test results, $\beta$ values for each test were calculated using Eqs. (2) and (3). Note that the column was assumed fixed at the bottom and the top instead of pinned at the top due to the constraint of the cap-beam and the other columns in the pier-bent observed from the test results. The resulting values for $\beta$ are presented in Table 1 for the six test cases for which residual plastic deformations were obtained. These values of $\beta$ were plotted by the scaled distance, $Z$ which is defined by $Z = w/x^{0.333}$ in Fig. 6 (Mays and Smith 1995). It was found that the value of $\beta$ for this type of

circular columns is 0.45 (i.e. mean value of 0.450 and standard deviation of 0.020 from the six samples considered).

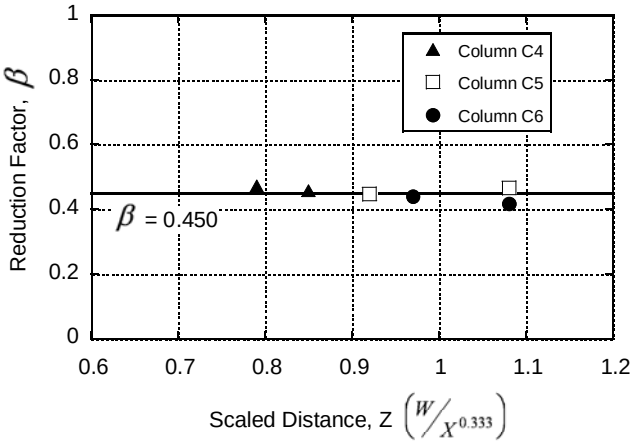


Fig. 6 Reduction factor

## FIBER-BASED DYNAMIC ANALYSIS

Fiber-based dynamic analyses were conducted to better understand the behavior of tested CFST columns when subjected to blast loading. Although an advanced FEM using solid elements or shell elements might be appropriate for capturing the localized behavior of the structural elements such as beam-column connections, frame models using a fiber-based model are more computationally effective to accurately capture the non-linear dynamic response of structures (Spacone et al. 1996a, 1996b). In the fiber-based model, a member section is divided into fibers in which the unidirectional stress-strain relationships of materials are assigned to represent the section characteristics, and the fiber-based model assumes that a plane section remains plane. The open-source OpenSees (2007) program was used to perform the fiber-based analyses in this research. Note that fiber-based model is suitable to capture flexural and axial behavior of the structure, but it cannot capture shear failure of the type observed in the previous tests of ductile reinforced concrete columns and steel jacketed non-ductile reinforced concrete columns (Fujikura and Bruneau 2011). None of the tested CFST columns considered here failed in shear, mostly due to the high shear capacity of steel tubes that are an integral part of CFST columns; rather, they failed in flexure. Therefore, using fiber-based analysis is a suitable approach to capture the residual plastic displacement observed during the test program.

## FIBER-BASED ANALYTICAL MODEL

Fig. 7 schematically shows the fiber-based analytical model of CFST columns for the blast loading tests. As shown in Fig. 7(a), the sections are divided into fibers for which the different materials are assigned different unidirectional stress-strain relationships. For a typical CFST, the steel tube was modeled as 64 discretized steel bar fibers, and the core concrete was modeled by 256 concrete fibers. The Menegotto-Pinto uniaxial constitutive model (Menegotto and Pinto 1973) was used for steel tubes. This model considers the hysteretic behavior of steel and accounts for Bauschinger effect. Core concrete was modeled using the Chang and Mander (1994) confined concrete model, modified by Waugh (2007) to increase its computational efficiency and numerical stability. Bruneau and Marson (2004) have shown that the confined concrete strength calculated by considering all the steel tube as concrete confinement significantly overestimates the capacity of CFSTs. Therefore, the effective

confinement stress, $f_l'$, was taken as 2.07 MPa (300 psi), which is the value used in the design of steel jacketed RC columns (Chai et al. 1991). The columns were modeled as discrete frames, as shown in Fig. 7(b). Discrete lumped masses were assigned to Nodes 2 to 16 as inertias to resist the blast loads. The gravity load corresponding to these masses was applied as a uniformly distributed load along column height. An axial force of 5.81 kN (1.31 kip) was applied to consider the loading from the cap-beam.

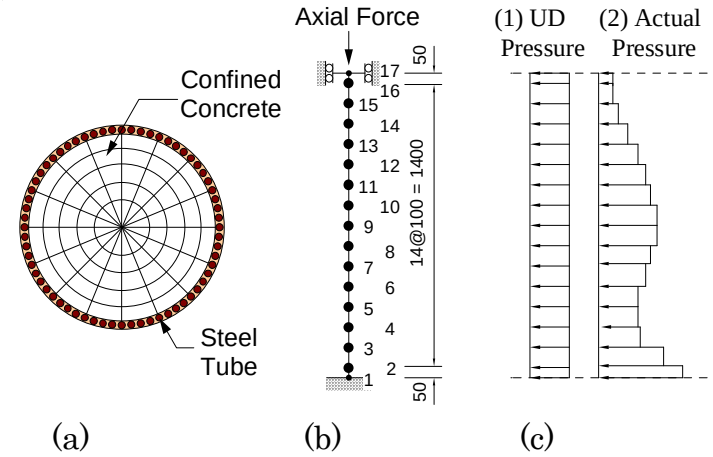


Fig. 7 Analytical model for blast loading tests: (a) cross section for fiber elements; (b) discretized model; (c) applied loading

Damping effects were considered through Rayleigh damping of 5 %. Modal analyses were conducted for the three CFST columns with different diameters (Columns C4, C5 and C6) to determine two modes of vibration for Rayleigh damping, and also to investigate their vibration properties, namely natural periods and mode shapes. The natural mode shapes of Modes 1, 3, 5, and 7 for Column C4 are shown in Fig. 8. These mode shapes are normalized by their corresponding effective masses. Note that because of fix-fix boundary conditions of the columns, anti-symmetric modes (such as Modes 2, 4 and 6) do not contribute the structural responses. Since, as shown in Fig. 8, Modes 1 and 3 are the dominant modes whose effective masses are respectively 69.0 and 13.2 %, Rayleigh damping was specified by these two modes. The vibration properties of Columns C5 and C6 were similar to the one of Column C4. The resulting natural period of the first mode was 5.13, 4.18, and 3.65 msec for Columns C4, C5, and C6, respectively.

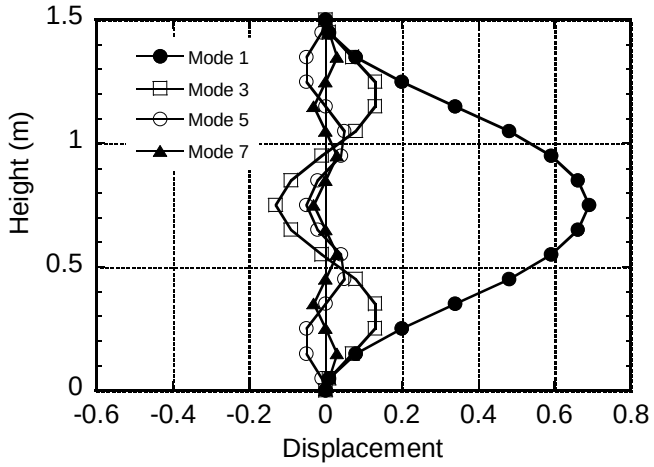


Fig. 8 Natural mode shapes of Column C4

To solve the nonlinear equilibrium equation, the Krylov-Newton algorithm provided by OpenSees (2007) was used. It is an iterative incremental solver based on the modified Newton method with Krylov subspace acceleration to calculate the next time step. This algorithm gives relatively faster and more robust convergence in general (Charlson and Miller 1998).

The first step of the fiber-based model analysis was to calibrate the model using the hysteretic material behavior of CFST columns. Here, quasi-static cyclic loading test data was used to verify the developed analytical model itself. Two CFST column specimens (CFST-34 and CFST-42) tested by Marson and Bruneau (2004) were used, and the analytically predicted behavior of these columns was compared with the experimentally obtained one. The comparison between the analytical and experimental hysteresis loops showed that the maximum base moment of CFST columns was predicted within 10 % accuracy when the drift exceeded 2 % with better than 5% accuracy from 3% drift to 5% drift, which was deemed satisfactory given that this calibration was performed on cyclic inelastic displacement histories having dozens of hysteretic loops (as typically used in such earthquake engineering tests), which challenged the numerical models more significantly than monotonically increasing lateral load application up to comparable drifts would have. Given that the rotations at the plastic hinges in the specimens obtained during the blast tests exceeded 2 % drift, the fiber-based model was confidently used for the blast analyses, allowing useful comparisons between results obtained using various analysis methods.

## APPLIED BLAST LOADINGS

Two profiles of blast loadings were applied in the blast pressure history analyses as shown in Fig. 7(c). One is (1) the uniformly distributed (UD) equivalent pressures, and the other is (2) the actual pressure distributions. The UD equivalent pressures were selected because they provide some preliminary basic understanding of the column response subjected to blast loading. This equivalent uniform pressure at time of $t$, $p_{eq}(t)$, is given by:

$$p_{eq}(t) = \frac{\int_0^H p(z,t)\,\phi(z)\,dz}{\int_0^H \phi(z)\,dz} \tag{5}$$

where $p(z,t)$ is pressure distribution along the height of a column at time $t$. The values of $p(z,t)$ were calculated using BEL, which was also used for the simplified analyses. Eq. (5) is the same format as Eq. (4) except for using $p(z,t)$ instead of $i(z)$. The analyses conducted using UD equivalent pressures were only performed for the three test cases with mid-height explosions (Test 3 on Column C4, Test 4 on Column C6, and Test 5 on Column C5) because the pressures actually applied to these columns during the tests were closer to symmetrically loading to the structure and are suited for modeling using UD loads due to this symmetry. Note that the equivalent uniform pressure, $p_{eq}(t)$, calculated by Eq. (5) takes pressure variation along a column into account based on the deflected shape of the column, $\phi(x)$. The resulting equivalent pressure history, $p_{eq}(t)$, for Test 3 on Column C4 is shown in Fig. 9 as an example. The time increment of each step in the pressure histories is 0.01 msec.

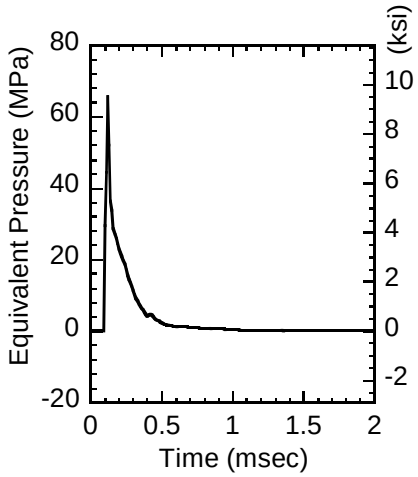


Fig. 9 Applied equivalent pressure history (Test 3 on Column C4)

The actual pressure profiles were also calculated by BEL. The blast pressures were obtained at 84 data points along the height of a column, and these pressures were averaged within each member (approximately five pressure points with each member) to reduce computational time. Fig. 10 shows the resulting applied blast pressures for Test 3 as an example. Fig. 10(a) presents a comparison of the blast pressure distributions along the height at two selected different time (t = 0.12 and 0.25 msec) from BEL compared with those applied in the analyses, and Fig. 10(b) shows the applied pressure histories for two selected elements which are Elem 1 and 8. This comparison indicates that the resolution of the averaged pressures within each member is satisfactory in terms of calculating the structural response. Note that the time in these figures starts at the initiation of the explosion. Also, note that a symmetric distribution of pressures is applied to the column, as shown in Fig. 10(a1), until the pressures are reflected on the ground. The reflected pressures on the ground are observed as higher pressures in the bottom elements as shown in Fig. 10(a2).

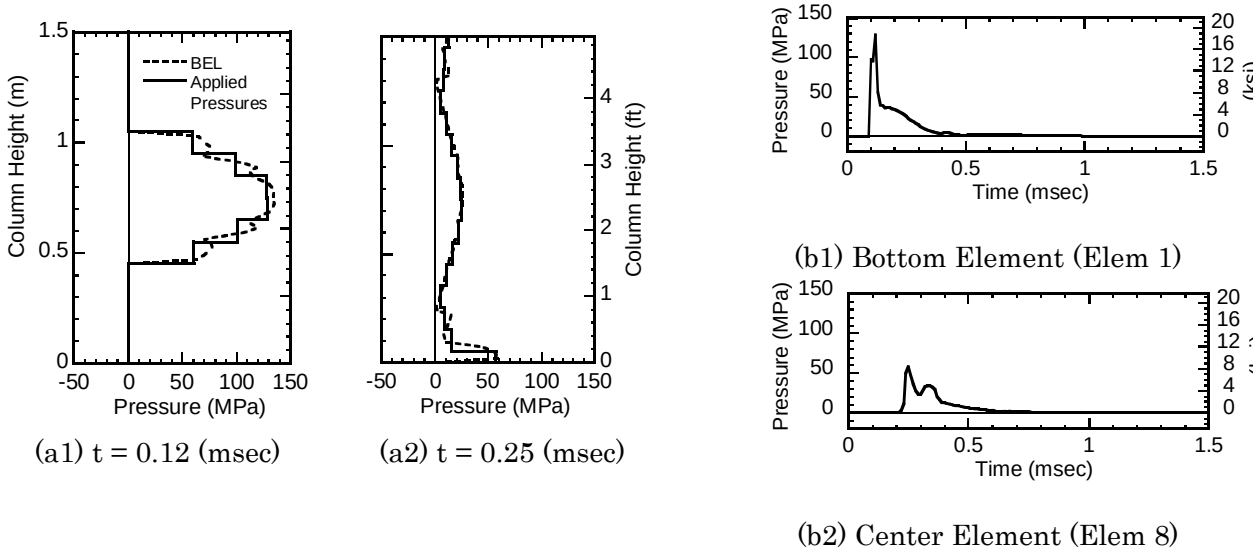


(a1) t = 0.12 (msec)

(a2) t = 0.25 (msec)

(b1) Bottom Element (Elem 1)

(b2) Center Element (Elem 8)

Fig. 10 Applied blast pressures for Test 3: (a) comparison of pressure distributions; (b) applied pressure histories

## STRUCTURAL RESPONSE OF CFST COLUMNS

Fig. 11 presents the analytical results of Test 3 for the mid-height explosion case when subjected to the UD equivalent pressures. These are acceleration and displacement distributions along the height of the column at three selected different times (t = 0.12, 0.60, and 1.04 msec). The time of 0.12 msec is shortly after the blast loading was applied and the largest accelerations are observed at this time. Almost no deformation is observed along the column at this time. The time of 0.60 and 1.04 msec, are arbitrarily selected to show that high frequency modes have developed in the acceleration response curves, similar to the mode shapes of the third and fifth modes, respectively, as shown in Fig. 8.

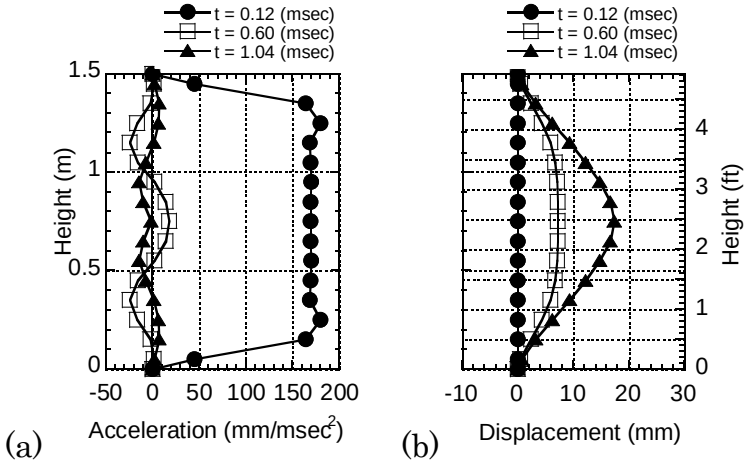


Fig. 11 Structural response distributions of Test 3 along height subjected to equivalent uniform pressures: (a) acceleration distribution; (b) displacement distribution

Fig. 12(a) compares the displacement history at mid-height under the UD equivalent pressures and actual pressures. In Fig. 12(a), when subjected to the UD equivalent pressures, the maximum displacement of 41.8 mm is observed at a time of 4.02 msec, of course much later than the end of the applied blast pressures (the blast pressure starts at a time of 0.10 msec, and the pressure duration is 0.16 msec). The displacement history subjected to the actual pressures is similar to the one observed in the UD equivalent pressure case. The reaction force history at base and top of the column is shown in Fig. 12(b1) and (b2) subjected to the UD equivalent pressures and actual pressures, respectively. As shown in Fig. 12(b1), the maximum reaction force of -303.8 kN is observed at a time of 0.15 msec that occurs before the end of the applied blast pressures. Note that the reaction forces at the base and top of the column are identical due to the symmetry of the column and applied blast pressure profiles. In Fig. 12(b1), there are some localized fluctuations of the reaction forces in the overall reaction force history curve. This is attributed to the high frequency modes of vibrations. For instance, the localized fluctuation of the reaction forces observed around a time of 0.60 msec in Fig. 12(b1) is caused by the acceleration shape at the time of 0.60 msec in Fig. 11(a). As shown in Fig. 12(b2), when subjected to the actual pressures, the reaction forces at the base and top of the column are identical up to 0.23 msec, but after that, the magnitude of the reaction force at the bottom increases significantly due to the reflected pressures on the ground applied around low-height of the column as shown in Fig. 10(a2).

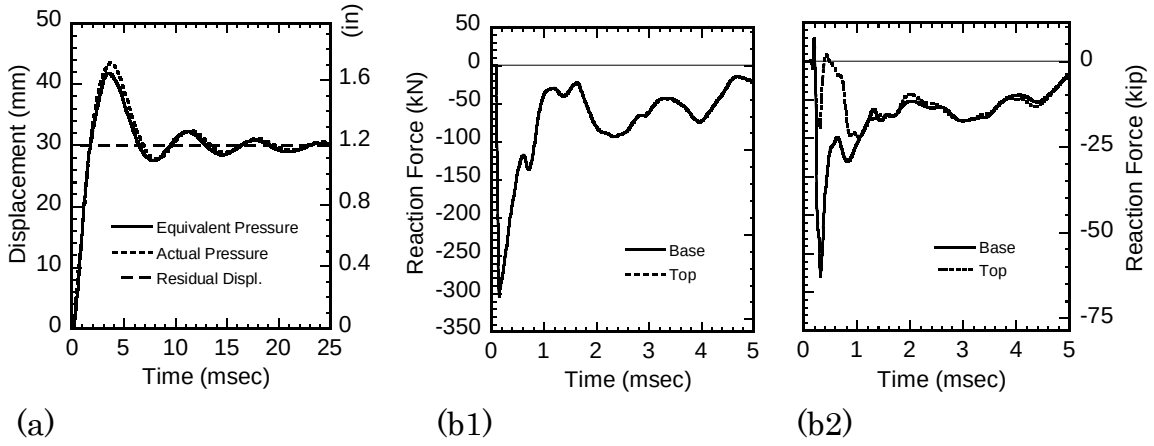


Fig. 12 Analytical results of Test 3 subjected to equivalent uniform and actual pressures:
(a) comparison of displacement history at mid-height;
reaction force history subjected to (b1) equivalent uniform pressures and (b2) actual pressures

## SHAPE FACTOR $\beta$

The shape factor $\beta$ was calibrated for the six columns to match the analytical results obtained from the fiber-based analyses with the experimental results. Table 2 summarizes the averaged resulting shape factor $\beta$ along with the one from the simplified analyses. For results using equivalent pressures, the $\beta$ values obtained from the analyses with 0.5 % damping ratio, in addition to the ones with 5 % damping ratio, are also presented in Table 2 to investigate the sensitivity of damping effects on the values of $\beta$. Because the analyses with 0 % damping ratio did not converge, a small damping ratio of 0.5 % was used for this purpose.

Table 2 Summary of shape factors from simplified analyses and fiber-based dynamic analyses

| | Simplified Analysis | Fiber-based Analysis | | |
|---|---|---|---|---|
| | | UD Equivalent Pressure | | Actual Pressure |
| Damping Ratio | 0 % | 0.5 % | 5 % | 5 % |
| Mid-height | 0.459 | 0.547 | 0.643 | 0.665 |
| Low-height | 0.441 | --- | --- | 0.561 |
| Total Ave. | 0.450 | --- | --- | 0.613 |

The $\beta$ value increases significantly, by about 18 %, for the fiber-based model with the increase of the damping ratio from 0.5 % to 5 % in the UD equivalent pressure profiles as shown in Table 2. To investigate this, Fig. 13 compares (a) the displacement history at column mid-height and (b) the reaction force history at column base corresponding to 0.5 % and 5 % damping ratios for the Test 3 case. Note that different $\beta$ factors, namely 0.564 for 0.5 % damping and 0.630 for 5 % damping,

were used for these analyses to match the analytical residual displacement with the one from the experiment, as shown in Fig. 13(a). As shown in Fig. 13(b), the resulting reaction force at the base of the column using 0.5 % damping ratio fluctuates with higher frequencies (i.e. at short periods in the range of 0.1 to 0.2 msec) whereas the reaction history curve using 5 % damping ratio is relatively smoother and has less effects of higher frequency modes. Since the 5 % Rayleigh damping was used based on the first and third modes of vibrations, the high frequency modes above the 3rd mode were less significant to the response. Therefore, using the Rayleigh damping in a fiber-based model has an effect, and can significantly reduce the structural response when subjected to blast loading.

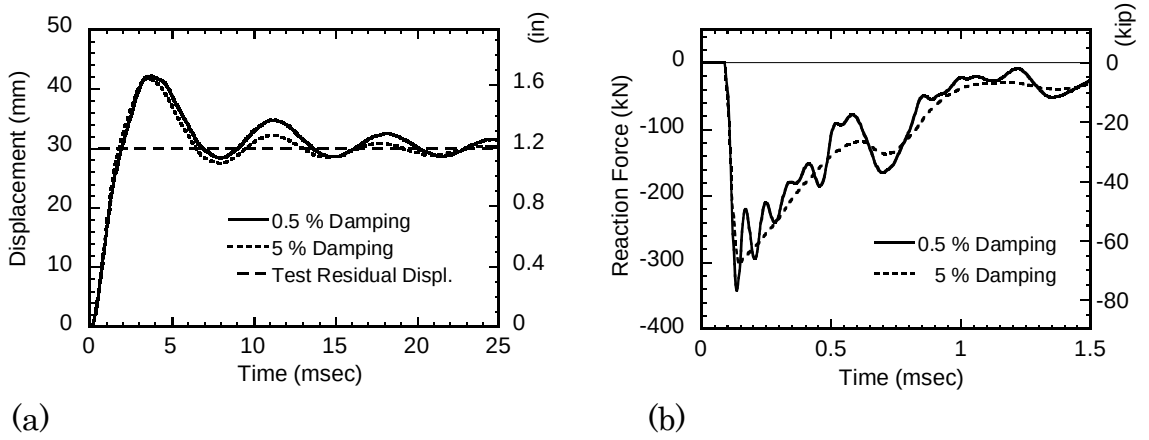


Fig. 13 Comparison of analytical results of Test 3 with different damping ratio: (a) displacement histories at mid-height; (b) reaction force histories at base

Beyond the above, it is also observed in Table 2 that using the actual pressure profile slightly increased the average $\beta$ value by 4 % over using the uniformly distributed equivalent pressures for the mid-height explosion case. When using actual pressure profiles, the average $\beta$ value for the low-height explosion cases is 15 % smaller than that for the mid-height explosion cases. This could be partly attributed to the reflected pressures on the ground computed by BEL. BEL assumes that the pressure reflects on the ground perfectly, but this was not the case in the experiments. Accordingly, the reflected pressures applied to the column close to the ground could be overestimated, resulting in the lower values of $\beta$ for the low-height explosion cases.

The results in Table 2 from the above analysis approaches (i.e. simplified analysis and fiber-based dynamic analysis) highlight the fact that the shape factor, principally intended to account for the reduction of blast pressures due to the circular shape of a column, is in fact unavoidably affected by some of the assumptions built in analytical models and methods applied. Therefore, it is important to use the value of $\beta$ that corresponds to the assumptions and conditions used for each analytical method.

## CONCLUSIONS

A multi-hazard bridge pier concept consisting of CFST columns to protect bridges from seismic and blast loading has been developed and experimentally validated. It is effective for blast resistance because breaching and spalling of concrete are prevented to occur in CFST columns. Blast tests showed that CFST columns of bridge pier specimens exhibited a satisfactory ductile behavior under blast loading.

This study also has showed that different values of $\beta$ (which reduces blast pressures when applied to a circular column) must be used with different analytical methods. Fiber-based dynamic

analyses showed that high frequency modes of vibration have some influence on the structural response when subjected to blast loading. It was also found that using Rayleigh damping with the fiber-based model can significantly reduce the structural response under blast loading due to the high frequency mode effects.

## ACKNOWLEDGMENT

This research was conducted by the University at Buffalo and was supported by the Federal Highway Administration under contract number DTFH61-98-C-00094 to the Multidisciplinary Center for Earthquake Engineering Research. This support is gratefully appreciated. However, any opinions, findings, conclusions, and recommendations presented in this paper are those of the writers and do not necessarily reflect the views of the sponsors. Special thanks are given to Dr. James C. Ray at the Eng. Research and Dev. Center of the USACE for his help and assistance in the logistics of the experiments.

## REFERENCES

*Bridge Explosive Loading version 1.1.0.3*. (BEL). (2004). US Army Corps of Engineers' Engineer Research and Development Center, Vicksburg, MS. (distribution limited to U.S. Government agencies and their contractors).

Bruneau, M., and Marson, J. (2004). "Seismic design of concrete-filled circular steel bridge piers", *Journal of Bridge Engineering*, 9(1), 24-34.

Chai, Y.H., Priestley, M.J.N., and Seible, F. (1991). *Flexural Retrofit of Circular Reinforced Concrete Bridge Columns by Steel Jackets*. Report Number SSRP-91/06, Department of Applied Mechanics and Engineering Sciences, University of California, San Diego.

Chang, G.A. and Mander, J.B. (1994). *Seismic Energy Based Fatigue Damage Analysis of Bridge Columns: Part I – Evaluation of Seismic Capacity*, Technical Report NCEER-94-0006, NCEER, State University of New York at Buffalo, Buffalo, NY.

Charlson, N.N. and Miller, K. (1998). "Design and Application of A Gradient-Weighted Moving Finite Element Code I: In One Dimension." *SIAM Journal of Scientific Computing*, vol. 19, No.3, pp.728-765, Society for Industrial and Applied Mathematics.

Federal Highway Administration (FHWA). (2003). *Recommendations for bridge and tunnel security*. Prepared by the Blue Ribbon Panel on Bridge and Tunnel Security, Washington, D.C.

Fujikura, S., Bruneau, M., and Lopez-Garcia, D. (2007). *Experimental Investigation of Blast Performance of Seismically Resistant Concrete-Filled Steel Tube Bridge Piers*, Technical Report MCEER-07-0005, MCEER, University at Buffalo, Buffalo, NY.

Fujikura, S. and Bruneau, M. (2011) "Experimental Investigation of Seismically Resistant Bridge Piers under Blast Loading", *Journal of Bridge Engineering*, 16(1), 63-71.

Marson, J., and Bruneau, M. (2004). "Cyclic testing of concrete-filled circular steel bridge piers having encased fixed-based detail." *Journal of Bridge Engineering*, 9(1), 14-23.

Mays, G.C., and Smith, P.D. (1995): *Blast effects on buildings*. Telford, London, UK.

Menegotto, M. and Pinto, E. (1973). "Method of analysis for cyclically loaded reinforced concrete plane frames including changes in geometry and non-elastic behavior of elements under combined normal force and bending." *Proceedings of IABSE Symposium*. Lisbon, Portugal.

*OpenSees*. (2007). Open System for Earthquake Engineering Simulation ver 1.7.5, Pacific Earthquake Engineering Research Center, University of California, Berkeley, CA.

Priestley, M.J.N., Seible, F., and Calvi, G.M. (1996). *Seismic Design and Retrofit of Bridges*, Wiley, New York, NY.

Smith, P.D., and Hetherington, J.D. (1994). *Blast and Ballistic Loading of Structures*, Butterworth-Heinemann.

Spacone, E., Filippou, F.C. and Taucer, F.F.(1996a). “Fiber Beam-Column Model for Non-Linear Analysis of R/C Frames: Part I. Formulation.” *Earthquake Engineering and Structural Dynamics*, Vol. 25, 711-725.

Spacone, E., Filippou, F.C. and Taucer, F.F.(1996b). “Fiber Beam-Column Model for Non-Linear Analysis of R/C Frames: Part II. Applications.” *Earthquake Engineering and Structural Dynamics*, Vol. 25, 711-725.

UFC. (2004). *Basic Guidelines for Chemical Hardening of New Military Facilities*. Unified Facilities Criteria UFC 3-340-13, Department of Defense, USA.

US Department of the Army (USDA). (1990). *Structures to Resist the Effects of Accidental Explosions*. Technical Manual TM 5-1300, Washington, DC.

Waugh J. (2007). Personal correspondence with writer. Department of Civil, Construction and Environmental Engineering, Iowa State University.

Williamson, E.B., and Winget, D.G. (2005). “Risk management and design of critical bridges for terrorist attacks.” *Journal of Bridge Engineering*, 10(1), 96-106.

Winget, D.G., Marchand, K.A., and Williamson, E.B. (2005). “Analysis and design of critical bridges subjected to blast loads.” *Journal of Structural Engineering*, 131(8), 1243-1255.